Supplementary information

From insulator to oxide-ion conductor by a synergistic effect from defect chemistry and microstructure: acceptor-doped Bi-excess sodium bismuth titanate $Na_{0.5}Bi_{0.51}TiO_{3.015}$

Fan Yang[1,*], Julian S. Dean[2], Qiaodan Hu[3], Patrick Wu[2], Emilio Pradal-Velázquez[2], Linhao Li[2] and Derek C Sinclair[2,*]

[1] Institute of Fuel Cells, School of Mechanical Engineering, Shanghai Jiao Tong University, 800 Dongchuan Road, Minhang District, Shanghai, 200240, P. R. China.

[2] Department of Materials Science and Engineering, University of Sheffield, Sir Robert Hadfield Building, Mappin Street, Sheffield, S1 3JD, UK.

[3] School of Materials Science and Engineering, Shanghai Jiao Tong University, 800 Dongchuan Road, Minhang District, Shanghai, 200240, P. R. China

*Corresponding authors. fanyang_0123@sjtu.edu.cn; d.c.sinclair@sheffield.ac.uk.

1. XRD patterns of other acceptor-doped $NB_{0.51}T$ ceramics

XRD patterns of $Na_{0.5}Bi_{0.51}Ti_{1-y}N_yO_{3.015-0.5y}$ (N = Sc, Al and Ga) ceramics are shown in Figs. S1-S3. Sc-doped $NB_{0.51}T$ ceramics are phase pure within the composition range investigated ($y \leq 0.05$). For Al- and Ga-doped $NB_{0.51}T$, peaks from secondary phases can be observed for y = 0.05 and 0.07, respectively.

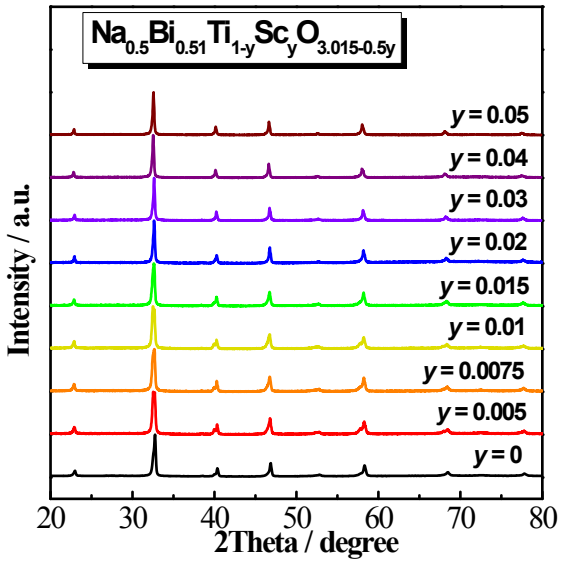

Fig.S1 XRD patterns of $Na_{0.5}Bi_{0.51}Ti_{1-y}Sc_yO_{3.015-0.5y}$ (y = 0, 0.005, 0.0075, 0.01, 0.015, 0.02, 0.03, 0.04 and 0.05) ceramics.

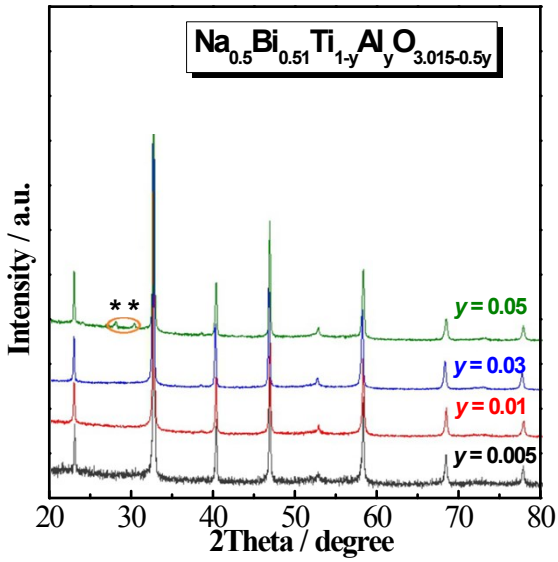

Fig.S2 XRD patterns of $Na_{0.5}Bi_{0.51}Ti_{1-y}Al_yO_{3.015-0.5y}$ (y = 0.005, 0.01, 0.03 and 0.05) ceramics. The star symbol indicates the presence of a secondary phase(s) for y = 0.05.

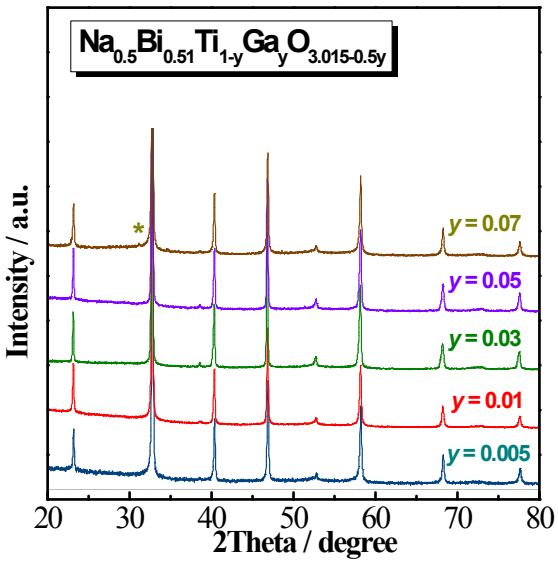

Fig.S3 XRD patterns of $Na_{0.5}Bi_{0.51}Ti_{1-y}Ga_yO_{3.015-0.5y}$ (y = 0.005, 0.01, 0.03, 0.05 and 0.07) ceramics. The star symbol indicates the presence of a secondary phase for y = 0.07.

2. Microstructure of $NB_{0.51}T$ and grain size distribution in Mg-doped $NB_{0.51}T$ ceramics

Undoped $NB_{0.51}T$ ceramics have uniform, small grains with an average grain size of ~ 1-2 μm (Fig. S4(a)). To ensure the thermally etched surface morphology is representative of the bulk, the grain structure was also observed as a cross-sectional, fracture surface (Fig.S4(b)). It also shows uniform, small grains and therefore confirms the surface grain structure is representative. In this work, the statistical analysis of the grain size is based on the thermally

etched surface for ease of comparison with that reported in the literature. For Mg-doped $NB_{0.51}T$ ceramics the grain size shows an increasingly broad distribution with increasing doping level (x), as well as an increase in the average value (Fig. S5).

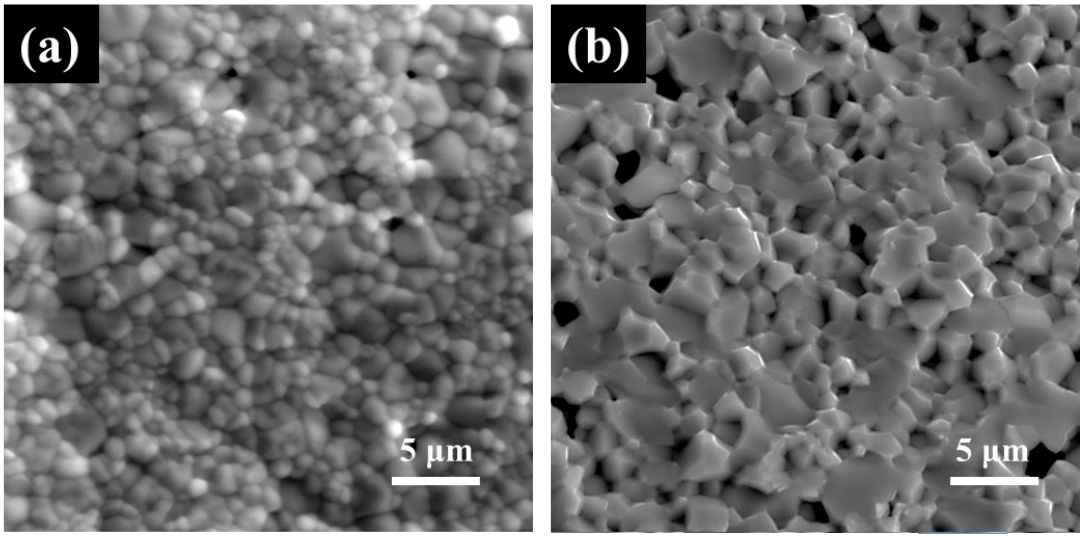

Fig.S4 SEM images of an $NB_{0.51}T$ ceramic: (a) thermal-etched surface and (b) fracture surface.

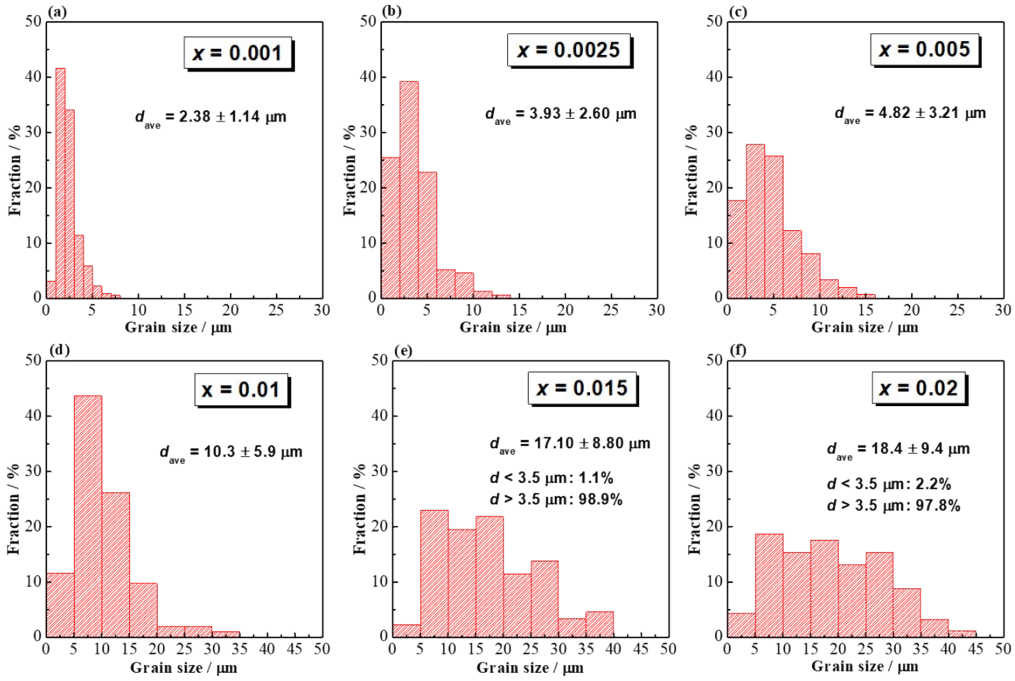

Fig. S5 Grain size distribution in $Na_{0.5}Bi_{0.51}Ti_{1-x}Mg_xO_{3.015-x}$ ceramics. (a) x = 0.001, (b) x = 0.0025, (c) x = 0.005, (d) x = 0.01, (e) x = 0.015 and (f) x = 0.02. Average grain size and its associated error is indicated in each figure.

3. Microstructure of other acceptor-doped $NB_{0.51}T$ ceramics

$NB_{0.51}T$ ceramics doped with other B-site acceptor-dopants show similar inhomogeneous distributions of large grains embedding in small grains at low doping levels, as shown in Fig.S6 for Zn and Fig.S7 for Sc. With increasing doping level *y*, the grain size of Sc-doped $NB_{0.51}T$ ceramics increases.

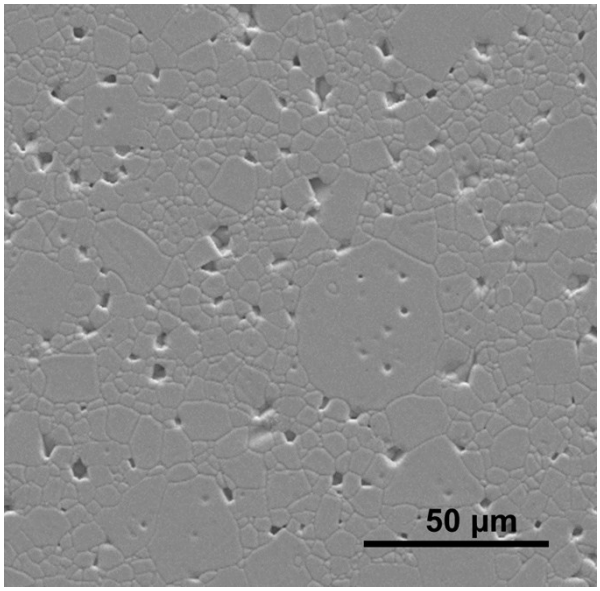

Fig. S6 SEM image of a thermally-etched surface of $Na_{0.5}Bi_{0.51}Ti_{1-x}Zn_xO_{3.015-x}$ (x = 0.005).

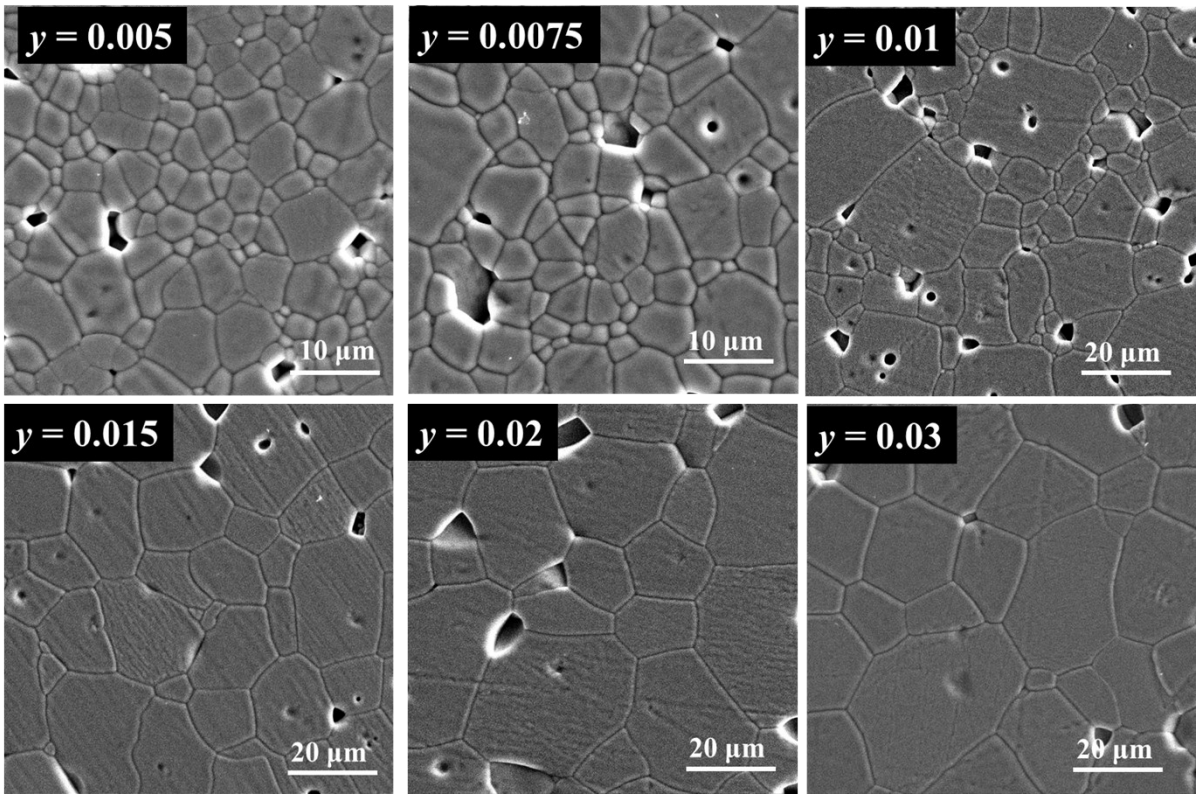

Fig.S7 SEM micrographs of thermally-etched surfaces of $Na_{0.5}Bi_{0.51}Ti_{1-y}Sc_yO_{3.015-0.05y}$ (y = 0.005, 0.0075, 0.01, 0.015, 0.02 and 0.03).

4. Compositional analysis of a thermally-etched Zn-doped $NB_{0.51}T$ (x = 0.005) ceramic

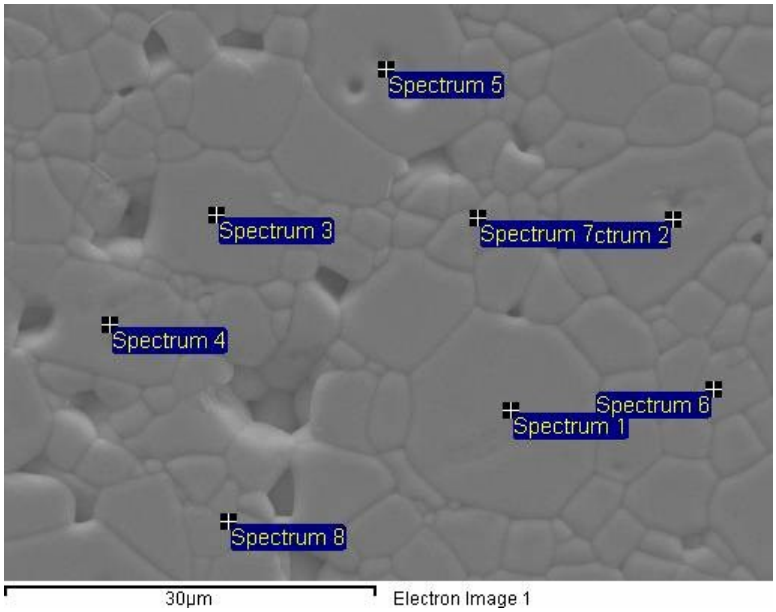

Table S1 Relative atomic percentage of cations in x = 0.005 $Na_{0.5}Bi_{0.51}Ti_{1-x}Zn_xO_{3.015-x}$ ceramics measured by EDS.

Position	Na	Bi	Ti	Zn
1	23.29	26.76	49.80	0.15
2	26.18	26.35	47.77	-0.30
3	25.12	26.46	47.97	0.45
4	23.45	26.91	49.08	0.55
5	24.74	26.26	48.90	0.10
6	25.37	26.17	47.86	0.60
7	22.04	27.21	50.75	0
8	24.12	26.80	49.34	-0.25
Average	24.29 ± 1.30	26.62 ± 0.36	48.93 ± 1.04	0.16 ± 0.35
Nominal	24.88	25.37	49.50	0.25

5. Bulk conductivity of Zn, Sc, Al and Ga-doped $NB_{0.51}T$ ceramics

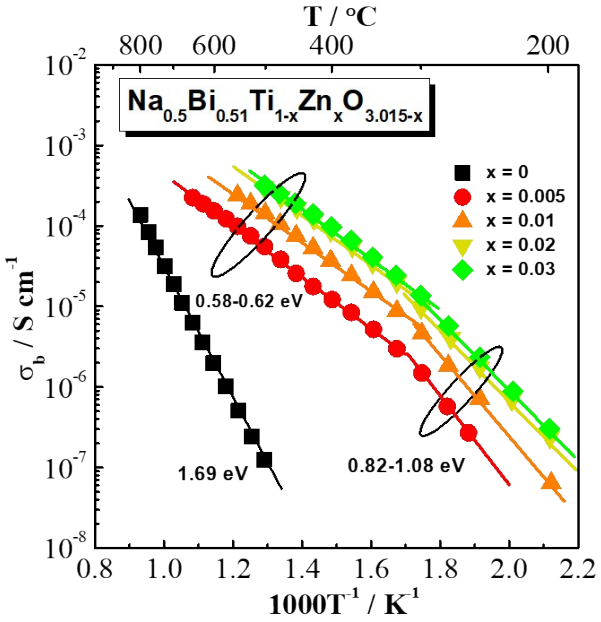

Fig.S8 Arrhenius plot of bulk conductivity, σ_b, for $Na_{0.5}Bi_{0.51}Ti_{1-x}Zn_xO_{3.015-x}$ ($x = 0$, 0.005, 0.01, 0.02 and 0.03) ceramics measured in air. Numbers in eV are the activation energies associated with σ_b.

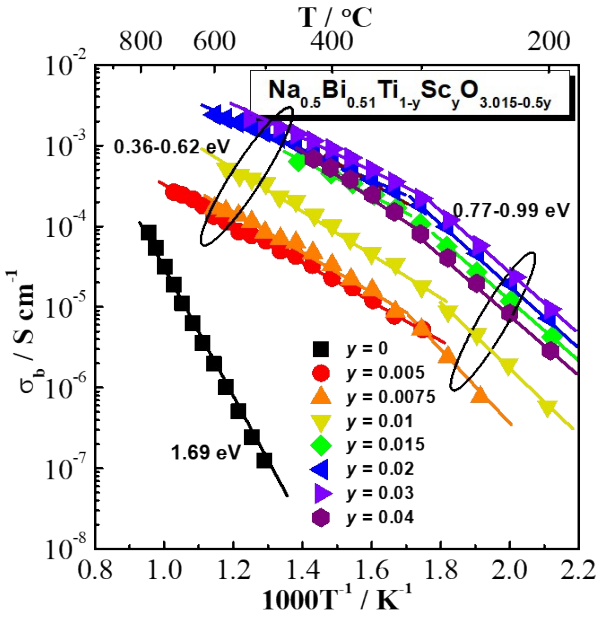

Fig.S9 Arrhenius plot of bulk conductivity, σ_b, for $Na_{0.5}Bi_{0.51}Ti_{1-y}Sc_yO_{3.015-0.5y}$ (y = 0, 0.005, 0.0075, 0.01, 0.015, 0.02, 0.03 and 0.04) ceramics measured in air. Numbers in eV are the activation energies associated with σ_b.

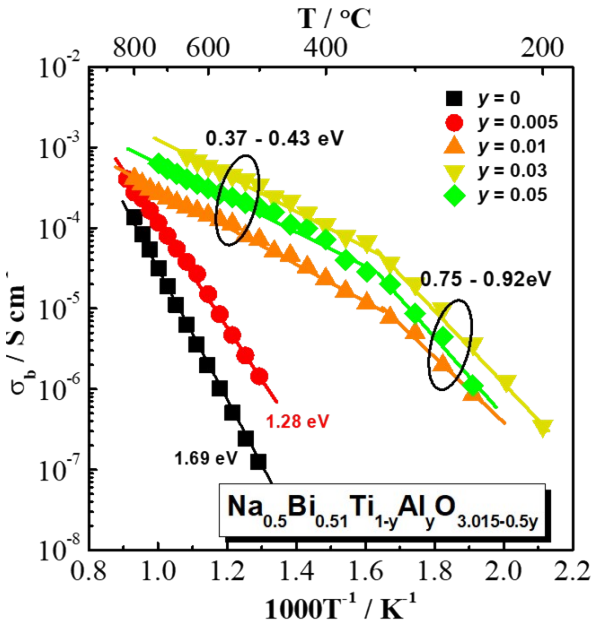

Fig.S10 Arrhenius plot of bulk conductivity, σ_b, for $Na_{0.5}Bi_{0.51}Ti_{1-y}Al_yO_{3.015-0.5y}$ (y = 0, 0.005, 0.01, 0.03 and 0.05) ceramics measured in air. Numbers in eV are the activation energies associated with σ_b.

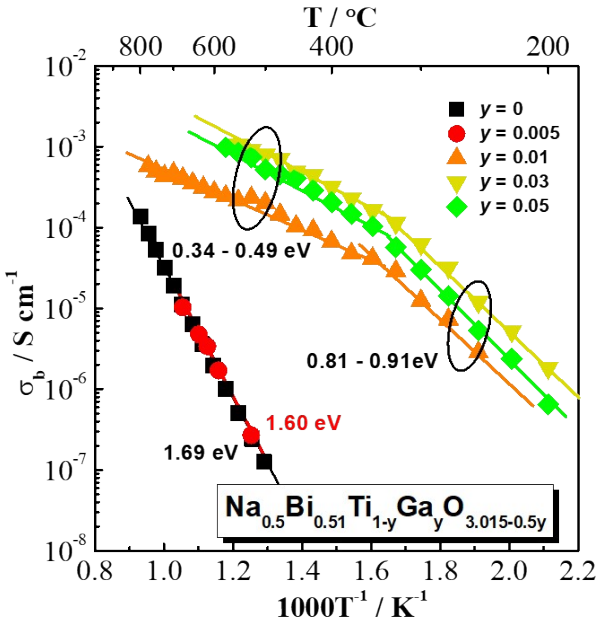

Fig.S11 Arrhenius plot of bulk conductivity, σ_b, for $Na_{0.5}Bi_{0.51}Ti_{1-y}Ga_yO_{3.015-0.5y}$ (y = 0, 0.005, 0.01, 0.03 and 0.05) ceramics measured in air. Numbers in eV are the activation energies associated with σ_b.

4. Dielectric properties of Zn, Sc, Al and Ga-doped $NB_{0.51}T$ ceramics

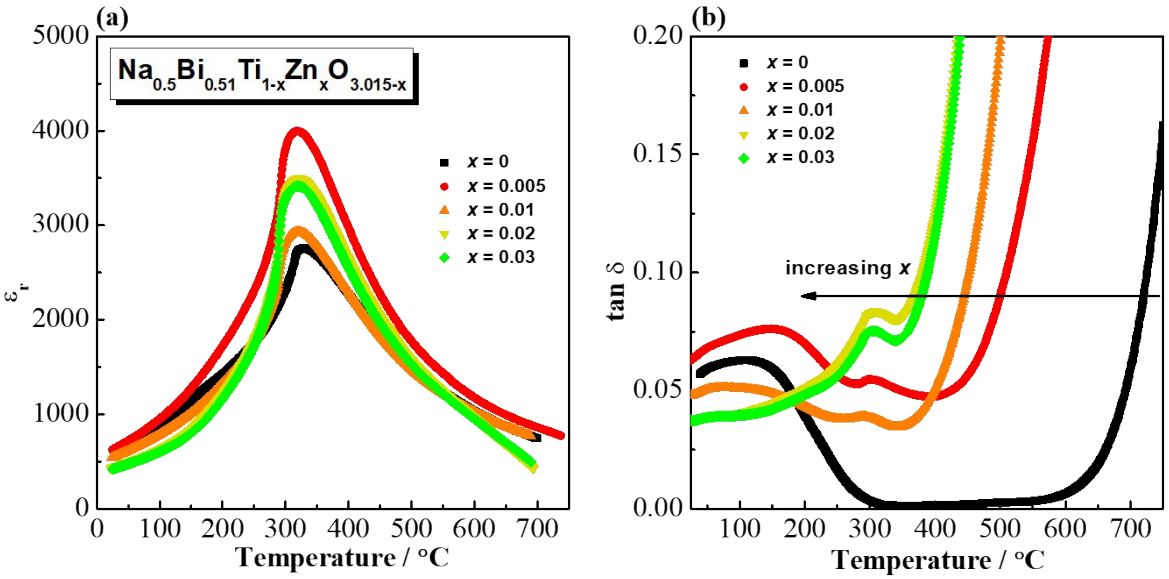

Fig.S12 Dielectric spectroscopy for $Na_{0.5}Bi_{0.51}Ti_{1-x}Zn_xO_{3.015-x}$ (x = 0, 0.005, 0.01, 0.02 and 0.03) ceramics: (a) permittivity at 1 MHz versus temperature and (b) dielectric loss, tan δ, (1 MHz) versus temperature.

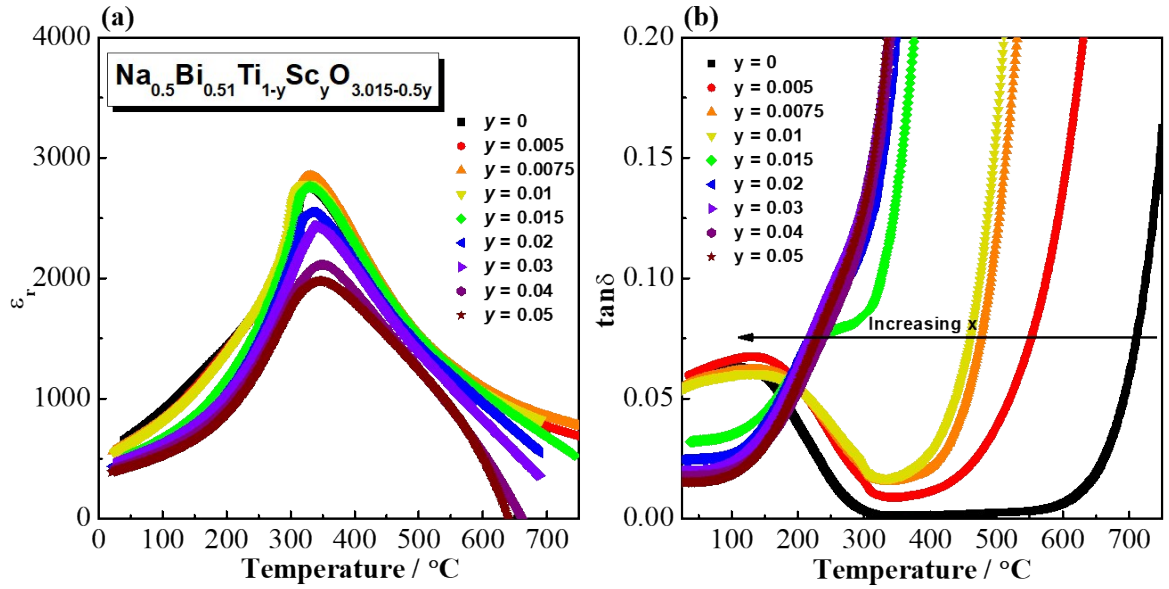

Fig.S13 Dielectric spectroscopy for $Na_{0.5}Bi_{0.51}Ti_{1-y}Sc_yO_{3.015-0.5y}$ (y = 0, 0.005, 0.0075, 0.01, 0.015, 0.02, 0.03, 0.04 and 0.05) ceramics: (a) permittivity at 1 MHz versus temperature and (b) dielectric loss, tan δ, (1 MHz) versus temperature.

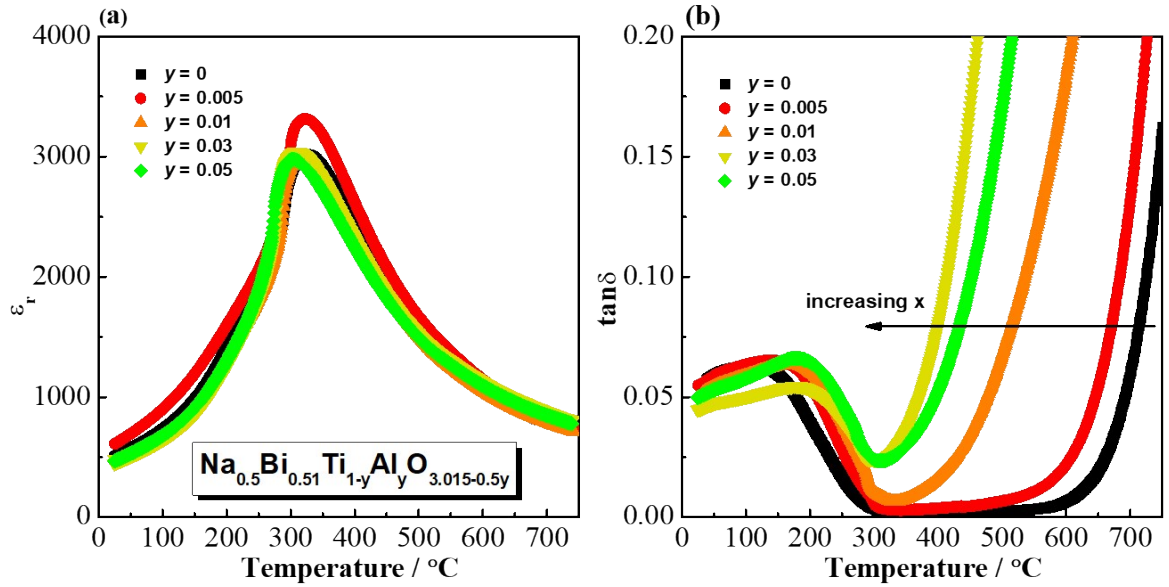

Fig.S14 Dielectric spectroscopy for $Na_{0.5}Bi_{0.51}Ti_{1-y}Al_yO_{3.015-0.5y}$ (y = 0, 0.005, 0.01, 0.03 and 0.05) ceramics: (a) permittivity at 1 MHz versus temperature and (b) dielectric loss, tan δ, (1 MHz) versus temperature.

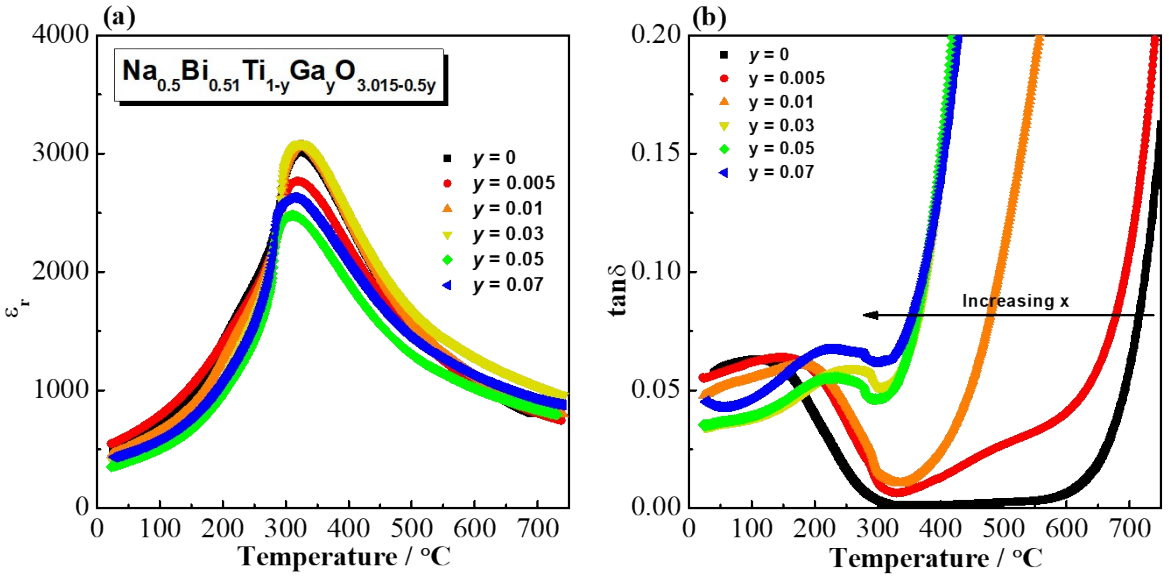

Fig.S15 Dielectric spectroscopy for $Na_{0.5}Bi_{0.51}Ti_{1-y}Ga_yO_{3.015-0.5y}$ (y = 0, 0.005, 0.01, 0.03, 0.05 and 0.07) ceramics: (a) permittivity at 1 MHz versus temperature and (b) dielectric loss, tan δ, (1 MHz) versus temperature.